THE EUROPEAN SOCIETY OF MEDICINE
Medical Research Archives, Volume 12 Issue 8

RESEARCH ARTICLE

Carbohydrate PL-M binds galectin-3 to inhibit SARS-CoV-2 viral entry into cells

Michelle C. Miller[1], Alben Sigamani[2], David Platt[3], Kevin H. Mayo[1]

[1] Department of Biochemistry, Molecular Biology and Biophysics, University of Minnesota, 6-155 Jackson Hall, 321 Church Street, Minneapolis, MN 55455, USA
[2] Carmel Research Consultancy Pvt. Ltd., Bengaluru, Karnataka 560025, India
[3] Pharmalectin India Pvt. Ltd., Rangareddy, Telangana 500039, India

OPEN ACCESS

PUBLISHED
31 August 2024

CITATION
Miller, MC., Sigamani, A., et al., 2024. Carbohydrate PL-M binds galectin-3 to inhibit SARS-CoV-2 viral entry into cells. Medical Research Archives, [online] 12(8). https://doi.org/10.18103/mra.v12i8.5616

DOI
https://doi.org/10.18103/mra.v12i8.5616

ISSN
2375-1924

ABSTRACT

Galectin-3 (Gal-3) binds to glycans on the spike protein S1 domain of the SARS-CoV-2 (Severe Acute Respiratory Syndrome Coronavirus 2) virus, thereby facilitating viral entry into cells. Because little is known about how to antagonize Gal-3 to block viral activity, we developed a pectin-derived polysaccharide of a(1-6)-**D**-mannopyranose (termed "ProLectin M" or PL-M) and studied its effect on Vero cells being infected with SARS-CoV-2 virus. Using this novel glycovirology approach, we demonstrated a significant reduction in viral load with no demonstrable cytotoxicity. We also evaluated the efficacy of PL-M in a randomized, double-blinded, placebo-controlled clinical study in 34 patients with mild to moderately severe COVID-19. Overall, treatment with PL-M significantly ($p = 0.001$) increased RT-PCR cycle counts for N and ORF genes on days 3 (Ct values 32.09 ± 2.39 and 30.69 ± 3.38, respectively) and 7 (Ct values 34.91 ± 0.39 and 34.85 ± 0.61, respectively) compared to placebo. From day 3 post-treatment, all subjects were RT-PCR negative for both genes in the PL-M treatment group, whereas placebo subjects remained positive. On the molecular level, our NMR studies show that PL-M binds relatively strongly to Gal-3, supporting the idea of an antagonist effect on the lectin. Gal-3 also binds strongly to sugar binding sites on the SARS-CoV2 virus spike protein S1 domain as evidenced by competitive lactose binding. In this regard, PL-M competes with the spike protein for binding to Gal-3 and thereby compromises viral entry into susceptible target cells, thus helping to explain our positive clinical effect from PL-M on the course of viral infection. This report provides a brief review of what is already known about PL-M and its effects on SARS-CoV2 virus, as well as new results on an expanded clinical trial with PL-M and NMR studies on the molecular mechanism of action of PL-M, Gal-3, and the SARS-CoV2 viral spike protein S1 from the Omicron variant.
Keywords: Galectin-3, ProLectin-M, SARS-CoV-2, Clinical Trial, NMR, Spike protein.

Abbreviations:

PLM: ProLectin-M
PLI: ProLectin I
NMR: nuclear magnetic resonance spectroscopy
SARS-COV-2: Severe Acute Respiratory Syndrome Coronavirus 2.
CRD: carbohydrate recognition domain;
Gal-3: human galectin-3
HSQC: heteronuclear single quantum coherence
MS: mass spectrometry;
NMR: nuclear magnetic resonance
PFG: pulsed field gradient.

Introduction:

The COVID-19 disease is caused by exposure to the severe acute respiratory syndrome coronavirus 2 (SARS-CoV-2).[1] During the recent COVID pandemic 2019 to ~2022, there were over 6.5 million deaths worldwide.[2] One of the difficulties in controlling this disease is that the viral genome, like other RNA viruses, mutates over time as it adapts to new hosts, thus resulting in multiple variants, e.g. alpha (B.1.1.7), beta (B.1.351), gamma (P.1), delta (B.1.617.2), and omicron (B.1.1.529 and its sub-lineages).[3-5] In particular, mutations appear in the receptor-binding (RBD) and N-terminal domains (NTD) of the spike protein S1 subunit, producing an enhanced infection rate, transmissibility, and/or virulence[3,6-9], as well as a decrease in the effectiveness of neutralizing antibodies and vaccines.[10,11]

During and after the COVID era, several vaccines were approved to reduce the severity of COVID-19 and reduce hospitalizations and death.[1,12] However, new variants of the SARS-CoV-2 virus are continually emerging[1,3,13] and threaten the ability to control viral infections among vaccinated populations.[14] Because of this, antivirals are likely the only viable solution to preventing transmission, either by inhibiting viral entry into cells or by inhibiting viral replication.

Viruses often exploit glycans on the cell surface by binding to them for cell entry. This is the case with SARS-CoV-2 virus where cell entry is initiated by interactions between the viral S protein RBD and glycans from ACE2 cell surface receptors.[15-18] This event is followed by fusion of the viral envelope with the host cell membrane and release of viral RNA into the host cytoplasm, after which the virus uses the replication machinery of the host cell to replicate its RNA and assemble new viral particles.[11,19] Because viral entry initiates this process[20], inhibiting it by blocking the virus or host-related components, such as RBD and NTD, seems to be the most effective way to prevent COVID-19.[6,21]

Viral entry into cells is mediated, in part, by galectins that are small b-galactoside binding lectins.[22-26] Among the known 15 or so human galectins, galectin-3 (Gal-3) promotes neutrophil infiltration and release of proinflammatory cytokines such as IL-6 and TNF-α[27], both of which are associated in patients with severe COVID-19[8,28,29] and contribute to inflammation and fibrosis that promote progression of severe COVID-19 and its long-term effects.[30] The Gal-3 carbohydrate recognition domain (CRD) binds to the S1 subunit NTD of the spike protein (S) to facilitate viral entry into cells.[23,24,26,31,32] In this regard, targeting Gal-3 is potentially useful as a viral therapeutic to inhibit SARS-CoV2 cell entry and associated inflammatory responses.

Structurally, Gal-3, the only chimeric galectin, has a collagen-like N-terminal tail (NT) and conserved carbohydrate recognition domain (CRD).[33] Of the 250 residues in human Gal-3, 110 comprise the NT with its numerous, functionally important Pro-Gly-Ala-Tyr/Trp repeat sequences.[34] As with all galectins, the Gal-3 CRD consists of 11 β-strands (β1 to β11) folded into a two sheet β-barrel, which is usually thought of as the primary functional domain of Gal-3.[35] Strands β1, β3, β4, β5, β6 and β10 form one of the β-sheets that has a convex surface termed the S-face, that is primarily responsible for binding carbohydrates[35], such as β-galactosides and α-galactosides[36-38], as well as negatively charged saccharides[60,61] and larger polysaccharides.[39] The other β-sheet (strands β2, β7, β8, β9 and β11) forms an opposing concave surface called the F-face with which the NT transiently interacts to modulate S-face carbohydrate binding.[34,40] The F-face itself interacts with some polysaccharides, like galactomannans.[41-43] Thus, the diversity of molecular interactions between carbohydrates and galectins is relatively broad.

ProLectin-M (PL-M) is a guar gum-derived carbohydrate composed of α-(1-6)-**D**-mannopyranose. In a small pilot trial, we showed PL-M reduces SARS-CoV-2 viral load in patients with severe COVID-19[44,45], as well as in an *in vitro* study on Vero cells.[46] Here, we report an expansion of that clinical study with orally-administered PL-M to 34 COVID-19 patients with mild to severe symptoms. For insight on the molecular level, we used NMR spectroscopy to show that Gal-3 binds strongly to PL-M, as well as to the viral spike protein S1, thus competitively inhibiting viral binding to cell surface glycans.[47] The Gal-3 CRD structure has been found in the N-Terminal Domain (NTD) of coronaviruses[7,17], including a high degree of structural similarity with it in SARS-CoV2, and like Gal-3, this domain in SARS-CoV2 binds *N*-acetylneuraminic acid (Neu5Ac), which is essential for viral entry into cells. This correlation may help explain why Gal-3 antagonist PL-M is effective at reducing SARS-CoV2 entry into cells.[48]

Methods and Materials

STUDY DESIGN AND OVERSIGHT

The efficacy of the study drug (Chewable Tablet Galactomannan, 1400 mg PL-M) was assessed in a randomised, double-blind, placebo-controlled clinical trial in ambulatory patients with mild to moderately severe COVID-19 infection. The study protocol was approved by the Institutional Ethics Committee (IEC) of ESIS Medical College and Hospital, Sanath Nagar, Hyderabad, India (ESIC Registration No: ECR/1303/Inst/TG/2019). As per regulatory standards, the study was registered with the Clinical Trials Registry-India (CTRI/2022/03/040757) on March 3, 2022. The study was conducted in accordance with the Declaration of Helsinki, the Good Clinical Practice guidelines, and local regulatory requirements. Prior to any trial-related activity, written informed permission from each participant was obtained. A total of 20 participants were identified, screened, and enrolled in this study. A paper-based case report form was used to capture all the clinical data.

INCLUSION AND EXCLUSION CRITERIA

The study involved 20 participants aged ≥18 years with mild to moderately severe COVID-19 infection who were willing to provide written informed permission and follow the trial guidelines. Participants were enrolled in the study if they had a recent rRT-PCR positive diagnosis (≤ 3 days) for COVID-19 infection with any of the following conditions: Ct value ≤ 25, hospitalisation for classical (CDC defined) COVID-19 symptoms (onset ≤ 5 days), and high-risk category of morbidity with SARS-CoV-2 infection. The exclusion criteria for participation included oxygen saturation levels (SpO2) ≤ 94% on room air, pregnant or breastfeeding women, active malignancy or chemotherapy, known allergies to any component of the study intervention, and pre-existing medical conditions that made the study protocol unsafe to follow. Participants who were receiving or had received any investigational COVID-19 treatment within 30 days before screening were also excluded from this study.

STUDY OBJECTIVE AND OUTCOME MEASURES

The objective of this study was to determine the efficacy of PL-M chewable tablets (1400 mg) as a galectin antagonist in patients with mild to moderately severe COVID-19 infection. The primary endpoint was to assess the change in the absolute count of the nucleocapsid gene and an increase in Ct value, estimated from COVID-19 samples taken from a nasopharyngeal swab. In addition, we intended to assess the cumulative incidence of adverse events (AEs), changes in clinical biochemistry, clinical haematology, changes in blood markers of inflammation and changes in COVID-19 antibody levels.

RANDOMIZATION AND TREATMENT

Patients who signed the informed consent form and met the eligibility criteria were enrolled in the study. Enrolled participants were randomly assigned to either the PL-M or placebo groups in a 1:1 ratio. An independent biostatistician provided a computer-generated assignment randomization list and blocks with varied block sizes to the investigators. Patients were given 1 tablet (either PL-M or matching placebo, 1400 mg) every hour for 7 days, with a maximum dose of 10 tablets per day because the viral replication cycle is 8-10 hours. Each participant was instructed to hold the tablet in their mouth for 1-2 minutes before dissolving and swallowing it. During mealtimes, such as breakfast, lunch, tea, and dinner, the subject was required to wait 30 minutes after the previous meal before taking the next tablet. This was done to avoid any potential reduction in blood glucose levels caused by the tablets' ability to impede absorption of carbohydrates taken during the meal.

STUDY INTERVENTIONS

The study interventions, PL-M (derived from gaur gum galactomannan) and placebo tablets (chewable), were manufactured at the GMP facility of Pharmalectin, Inc. in Pune, Maharashtra. All the study interventions were identical in appearance, shape, colour, packaging, and texture.

STUDY PROCEDURES

At all visits on days 1, 3, and 7, nasopharyngeal/oropharyngeal swab samples were taken from each patient to test for COVID-19 positivity using the RT-PCR method. Swab samples were transported to the research facility for Ct value analysis for the open reading frame (ORF) and nucleocapsid (N) protein genes. Throughout the analysis, all laboratory workers remained blind to treatment allocation. RNA extractions were performed using the QIAamp Viral RNA mini kit (#52904, Qiagen) according to the manufacturer's standard protocol. A sample was considered negative if no Ct value was obtained and no amplification curve was observed, or if the Ct value for all three targets was > 29. At each visit, clinical symptoms, adverse events (AEs), and concomitant medicines were recorded. Patient safety was assessed both at the beginning and completion of the trial (day 7). Changes in vital signs and laboratory tests such as haematology, and serum biochemistry were evaluated as part of the safety assessment. Patients were monitored for 28 days from the day of randomization.

rRT PCR:

The extracted RNA was analysed using TRUPCR® SARS-CoV-2 RT qPCR KIT V-2 (#3B3043B Black Bio Biotech). In the real-time RT-PCR assay, 2 target genes including ORF and N genes were evaluated. Ct values obtained from a series of 5 template DNA dilutions of at least 3 separate samples were graphed on the y-axis versus the log of the dilution on the x-axis to measure the efficiency of the PCR. The Ct values assumed by the following equation were used to determine the logarithm of the recombinant gene copy numbers from: Ct = slope log (Gene Copy Number) + 1, where 1 acts as the standard curve's intercept.

STATISTICAL ANALYSIS

A total of 34 subjects were randomized, and no formal sample estimation was undertaken. Ct values and absolute copy numbers were compared using a parametric, unpaired repeated t-test with Welch's correction or a non-parametric Mann Whitney U test. A two-tailed, $p<0.05$, was considered statistically significant.

NMR SPECTROSCOPY

Nuclear Magnetic Resonance (NMR) studies were carried out at 30°C on a Bruker 850 MHz spectrometer outfitted with a H/C/N triple-resonance probe and an x/y/z triple-axis pulse field gradient unit. A gradient sensitivity-enhanced version of two-dimensional ^{1}H-^{15}N HSQC (Heteronuclear Single Quantum Coherence) was applied with 256 (t1) x 2048 (t2) complex data points in nitrogen and proton dimensions, respectively. Raw data were converted and processed by using NMRPipe and were analyzed by using NMRview.[49,50] Uniformly ^{15}N-labeled galectin-3 (Gal-3) was dissolved at a concentration of 20 μM in a 20 mM potassium phosphate buffer at pH 6.9, prepared with a 95% H2O/5% D_2O mixture. To explore the binding of PL-M and its separate polysaccharide components (galactomannans AG and R) to Gal-3, ^{1}H–^{15}N HSQC NMR measurements were performed. The ^{1}H and ^{15}N resonance assignments of recombinant human Gal-3 were reported earlier.[51]

Chemical shifts are internally referenced to DSS (4,4-dimethyl-4-silapentane-1-sulfonic acid), and chemical shift differences ($\Delta\delta$) were calculated as $[(\Delta^{1}H)^2 + (0.25\,\Delta^{15}N)^2\ ]^{1/2}$. Solution conditions were 20 mM potassium phosphate, pH 6.9.

Results

Previously, we reported that PL-M is effective at inhibiting SARS-CoV-2 viral entry into cells.[46] For this, we used two approaches: 1) pre-treated cultured cells with PL-M at various concentrations prior to infecting cells with the virus, and 2) first infected the cells with virus and then treated the cells with PL-M at various concentrations. In the first approach, the anti-viral assay for SARS-CoV-2 showed that PL-M rendered nearly 99% reduction in viral RNA copy number compared to control when the PL-M concentration was > 7 mg/mL (Figure 1A). In the second approach, PL-M treatment of infected cells reduced viral load ~40% at >7 mg/mL (Figure 1B). In either instance, viral particles were reduced from $10^{6.9}$ to $10^{5.1}$ and from $10^{6.9}$ to $10^{5.5}$ before and after PL-M treatment, respectively.[46] The MTT assay showed that PL-M was non-cytotoxic for cells at concentrations up to at least 100 µg/mL, with CC_{50} values >100 µg/mL.[46]

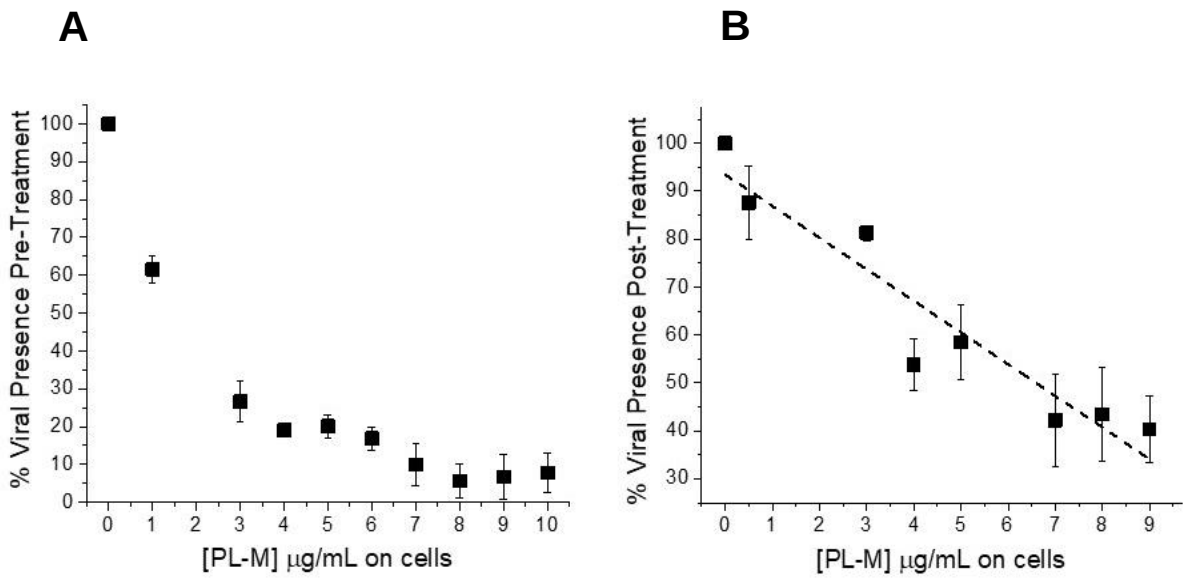

Figure 1. Two protocols to treat viral infection in Vero cells. In protocol 1, Vero cells were first treated with PL-M prior to infection with SARS-CoV-2. DMSO was the control. In protocol 2, Vero cells were cultured with SARS-CoV-2 virus prior to treatment with PL-M. The dashed line in **B** is shown as a visual aid. Data are the mean ± SD of triplicate experiments.

In an initial COVID-19 clinical trial with PL-M, we screened 20 patients (10 placebo and 10 PLM treated) with mild to severe COVID-19 disease, and divided them into two groups.[45] Each group had 10 participants with an average age of 36.60 ± 8.40 years (placebo) and 41.60 ± 6.42 years (PL-M group). In each group, SARS-CoV-2 RT-PCR tests were performed on days 0, 3, and 7. Detection of SARS-CoV-2 viral RNA is usually achieved by real-time RT-PCR of two target genes, the open reading frame (ORF) of 1ab and the nucleocapsid protein (N). RT-PCR cycle counts for N and ORF genes in both groups increased during the treatment period (days 3-7), with RT-PCR cycle counts being significantly higher in the PL-M treatment group (cycle counts 29.26 ± 3.33 and 33.10 ± 0.0 in days 3 and 7, respectively; p = 0.001). All participants in the PL-M group turned RT-PCR negative from day 3 onwards, whereas none of the participants in the placebo group became RT-PCR negative until day 7.

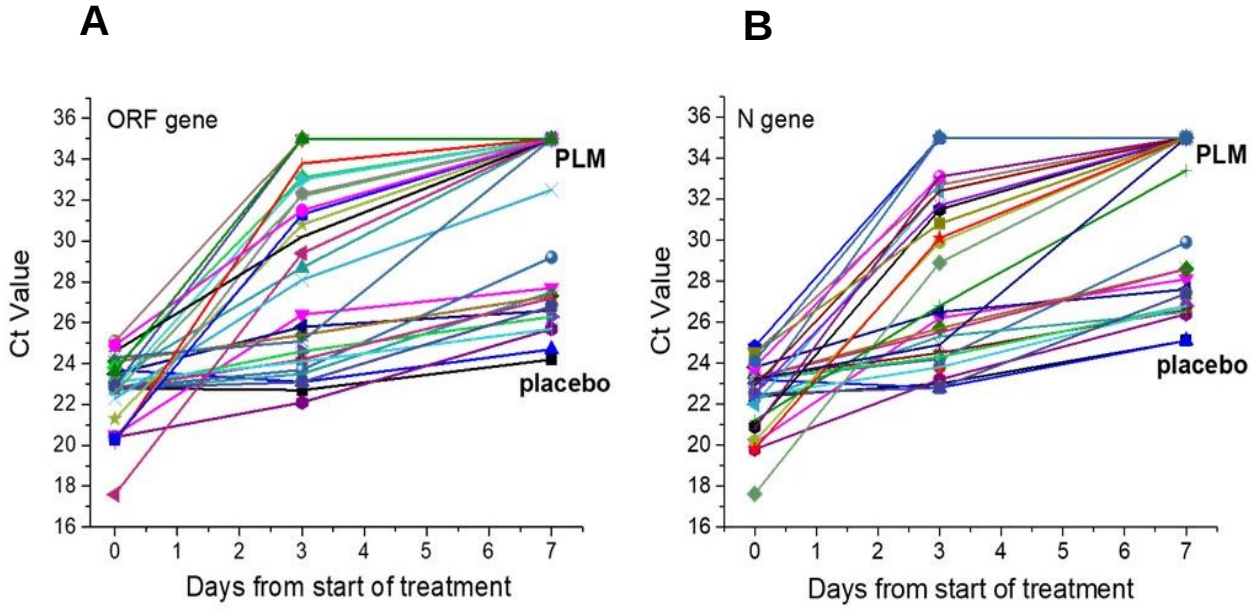

We recently expanded this COVID clinical trial to 34 patients (17 placebo and 17 PLM treated). These results paralleled those obtained in the initial trial described above. Figure 2 and Table 1 show that on day 7, all participants in the PL-M treated group had cycle counts above the targeted cut-off value of 29, whereas the majority of participants (16 or 94.12%) in the placebo group had cycle counts below the targeted cut-off value.

Figure 2. RT-PCR profiles of (**A**) N gene, (**B**) ORF gene, (**C**) N gene showing changes in individual patients along with average values and SDs, and (**C**) ORF gene showing changes in individual patients along with average values and SDs. Changes in Ct values in placebo and PL-M groups. RT-PCR profiles of N and ORF genes detected SARS-CoV-2 in COVID-19 patients on days 0, 3 and 7.

Table 1. RT-PCR cycle counts for N and ORF gene at different visits.

COVID tests	**RT-PCR cycle counts (Ct values)**		
N gene	**Control group (n = 34)**	**PL-M group (n = 34)**	**p-value**
Day 0	22.65 ± 0.263	22.3 ± 0.242	0.288
Day 3	24.4 ± 0.302	31.7 ± 0.702	0.001
Day 7	27.2 ± 0.304	34.9 ± 0.094	0.001
ORF gene			
Day 0	22.85 ± 0.242	22.5 ± 0.484	0.393
Day 3	24.18 ± 0.281	31.7 ± 0.68	0.001
Day 7	26.7 ± 0.287	34.86 ± 0.135	0.001

Having established the *in vitro* and *in vivo* effectiveness of PL-M against SARS-CoV-2 infectivity[44-46], we sought insight on the molecular level as to how PL-M functions against the virus. We hypothesized that PL-M binds to and antagonizes Gal-3, which is known to interact with the SARS-CoV-2 viral spike protein to promote viral entry into cells.[44-46] To validate this proposal, we used NMR spectroscopy to assess binding interactions between PL-M and Gal-3, as well as between Gal-3 and SARS-CoV-2 spike protein S1 subunit.

Gal-3 binds to PL-M. HSQC NMR spectra of ^{15}N-labeled Gal-3 were measured as a function of PL-M concentration (0.3, 0.6, 1.2, 2.4 and 4.8 mg/mL). A ^{1}H-^{15}N HSQC spectral expansion is shown in Figure 3A for ^{15}N-Gal-3 in the absence (peaks in black) and presence (peaks in red) of 1.2 mg/mL PL-M. During the titration, Gal-3 resonances were differentially chemically shifted and reduced in intensity (broadened), with some peaks becoming so broadened by the end of the titration that they cannot be observed. This observation alone demonstrates that Gal-3 binds to PL-M and indicates that the overall structure of Gal-3 is not significantly perturbed upon binding. Moreover, the fact that resonances are significantly broadened and minimally chemically shifted, PL-M binding to Gal-3 falls in the intermediate exchange regime on the chemical shift time scale, suggesting that the equilibrium dissociation constant (K_D) lies in the 2 μM to 100 μM range.[52] The extent of resonance broadening is related to binding affinity and stoichiometry, in addition to any binding-induced changes in internal motions and conformational exchange. Therefore, one might look at this as binding avidity, or the net ability of PL-M to bind to Gal-3. Alternatively, or in addition, the apparent broadening could result from multiple binding modes given the heterogeneous nature of the PL-M polysaccharide. Either way, Gal-3 binds relatively strongly to PL-M.

Even though PL-M binding-induced ^{15}N-Gal-3 chemical shift changes, $\Delta\delta$, are relatively small, they are useful to assess the binding epitope on the lectin. Figure 3B plots ^{15}N-Gal-3 chemical shift changes, $\Delta\delta$, vs. the amino acid sequence of Gal-3. The most shifted resonances arise from Gal-3 CRD residues in β-strands 3, 4, 5 and 6 that comprise the S-face β-sheet of the β-sandwich to which the β-galactoside lactose binds, as illustrated in Figure 3C, which shows the structure of the Gal-3 CRD (pdb access code: 1A3K) with the most shifted residues highlighted. This indicates that the PL-M binding epitope on Gal-3 is within the canonical sugar binding domain on the S-face of the CRD. Chemical shift changes within the N-terminal tail (NT) (residues 1-111) most likely result from PL-M binding-induced allosteric effects on the CRD F-face and modulation of interaction dynamics between the NT and CRD F-face.[40] Figure 3D plots chemical shift changes averaged over all Gal-3 resonances vs. the concentration of PL-M with the 50% saturation point in the plot falling at ~1 mg/mL. However, because Gal-3 binding falls in the intermediate exchange regime, one cannot accurately determine binding affinity/avidity (or stoichiometry), other than the equilibrium dissociation constant, K_d, falling in the ~2 μM to ~100 μM range (Williamson, 2013).[52] Essentially the same binding results were observed with PL-M and ^{15}N-labeled truncated Gal-3 CRD that is devoid of its N-terminal tail (data not shown).

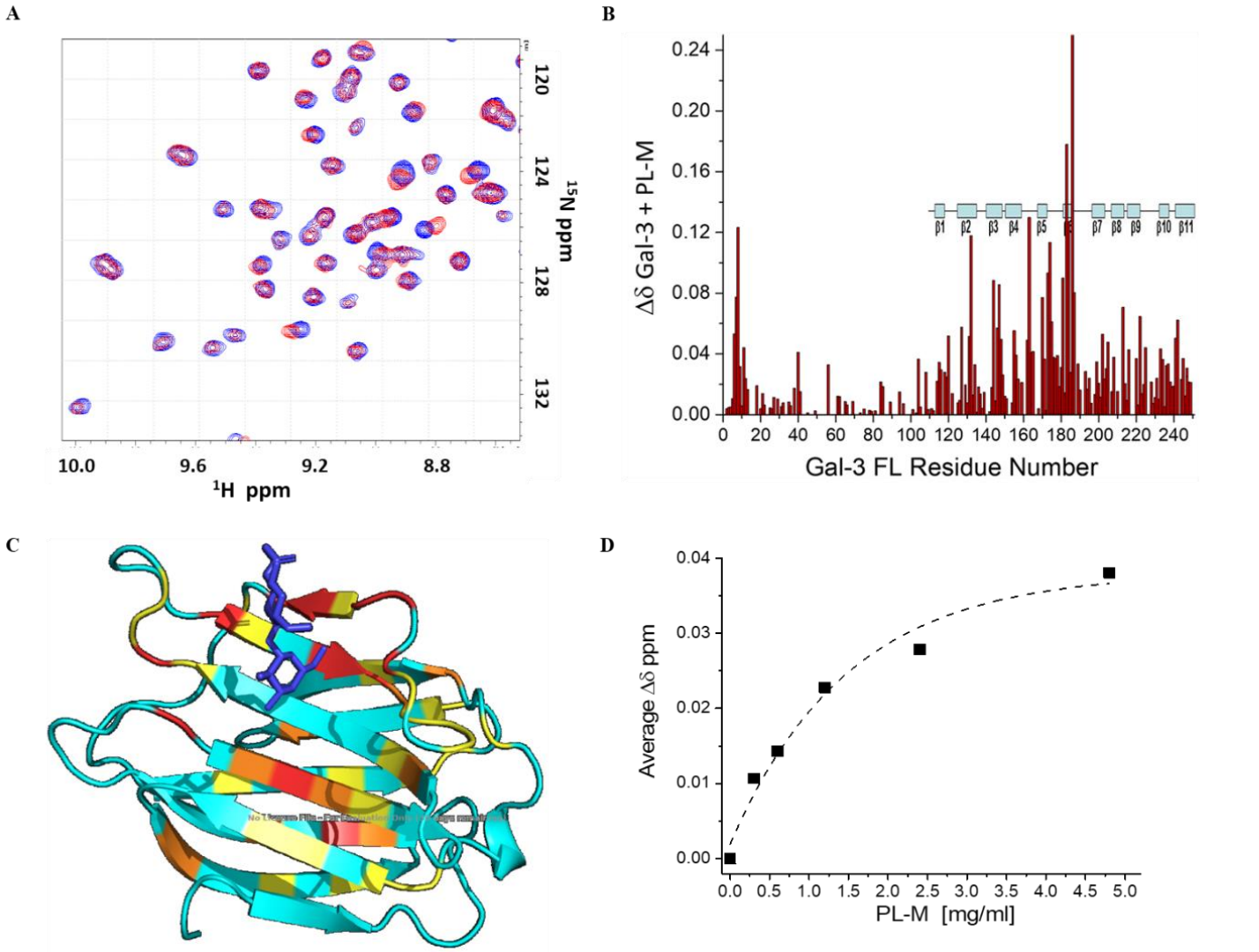

Figure 3. (**A**) ^{15}N HSQC expansions are overlaid for ^{15}N-labeled Gal-3 (20 μM) in the absence (black peaks) and presence of 1.2 mg/ml PL-M (red peaks). (**B**) Chemical shift map (Δδ vs. the sequence of Gal-3) for PL-M binding to Gal-3. (**C**) Crystal structure of Gal-3 (pdb 1A3K)[53] shows largest Δδ values in red (> 2SD above Δδ average), orange (1SD to 2SD), yellow (average and 1SD), and aqua (< average). (**D**) Averaged Δδ is plotted vs PL-M concentration. Data were exponentially fitted as shown by the dashed line.

Gal-3 binds to SARS-CoV-2 S1 Spike Protein. To further validate our hypothesis, we used NMR spectroscopy to assess interactions between the viral spike protein S1 (~32kDa) and Gal-3, both to the full-length lectin (~29kDa) and to its truncated CRD form (~15kDa). HSQC NMR spectra of ^{15}N-labeled full length Gal-3 (Gal-3 FL) were measured as a function of spike protein concentration (0.2, 0.4, 1, 2, 4 and 10 μM). ^{15}N-^{1}H HSQC spectra are shown in Figure 4A for ^{15}N-Gal-3 FL in the absence (peaks in black) and presence (peaks in red) of 1 μM spike protein. As with PL-M binding, Gal-3 resonances are differentially chemically shifted and reduced in intensity (broadened), with some peaks becoming so broad by the end of the titration that they could not be observed, demonstrating that Gal-3 FL binding to the spike protein occurs in the intermediate exchange regime on the chemical shift time scale with an apparent K_D lying in the 2 μM to 100 μM range. Figure 4B shows that Gal-3 FL resonance broadening is about 50% at 1 μM spike protein, with effects within the NT and CRD occurring to the same extent. This suggests that the NT itself, and not only the CRD, may play a role in binding to the spike protein.

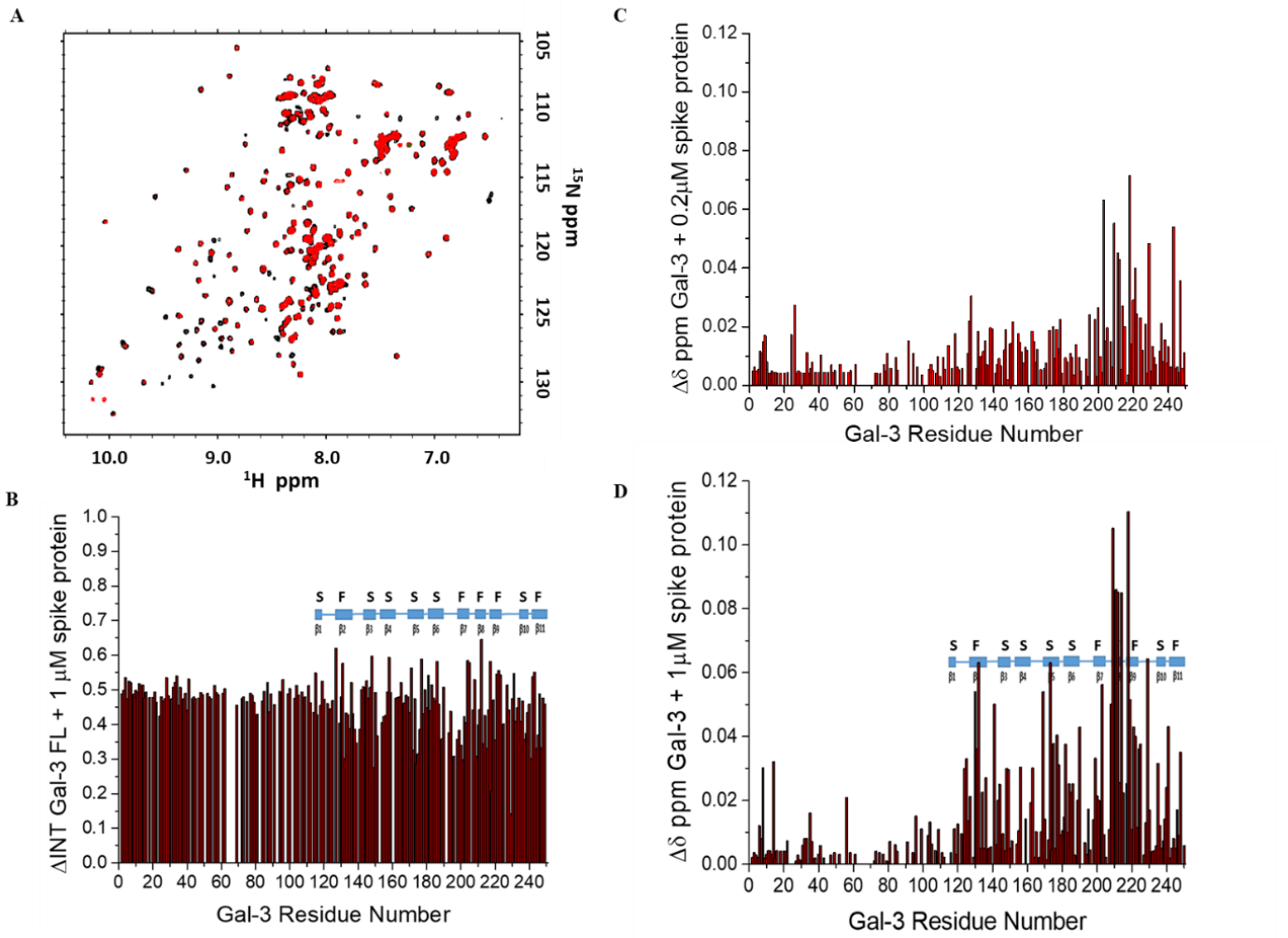

Figure 4. (**A**) ^{15}N HSQC spectra are overlaid for Gal-3 (20 μM) in the absence (black peaks) and presence of 1 μM S1 spike protein (red peaks). (**B**) ΔINT values show Gal-3 resonance broadening upon binding to spike protein. (**C**) Δδ values calculated in the absence and presence of 0.2 μM spike protein are plotted vs. the Gal-3 residue number. (**D**) Δδ values calculated in the absence and presence of 1 μM spike protein are plotted vs. the Gal-3 residue number.

Figure 4C plots ^{15}N-Gal-3 FL chemical shift changes, Δδ, vs. the amino acid sequence of Gal-3 at the spike protein concentration of 0.2 μM. Here, it is important to note that while canonical sugar binding S-face residues are chemically shifted, the most shifted resonances actually arise from Gal-3 residues within β-strands 2, 7, 8 and 9 that comprise the F-face β-sheet to which the NT transiently interacts.[40] This indicates that the initial interaction site with the spike protein is primarily on the F-face. However, at 1 μM spike protein (Figure 4D), binding to the Gal-3 FL CRD S-face becomes more enhanced as one might expect.

HSQC spectra of ^{15}N-labeled truncated Gal-3 CRD were also measured as a function of spike protein concentration (0.2, 0.4, 1, 2, 4 and 10 μM). ^{15}N-^{1}H HSQC spectra are overlaid in Figure S1A for ^{15}N-Gal-3 in the absence (peaks in black) and presence (peaks in red) of 1 μM spike protein. Even though it appears that binding of both Gal-3 FL and truncated Gal-3 CRD to the spike protein occur to similar extents, as reflected in changes in resonance broadening (Figure S1B), Δδ values for truncated Gal-3 CRD at 1 μM spike protein are relatively small and more scattered throughout the CRD, both S- and F-faces (Figure S1C), compared to Gal-3 FL. This suggests that Gal-3 FL with its N-terminal tail (NT) provides the better binding epitope(s) for interactions with the spike protein.

Figure S1D plots ΔINT values averaged over all Gal-3 resonances for both Gal-3 FL and Gal-3 CRD vs. the concentration of the spike protein. In both cases, broadening plateaus out at ~4 μM spike protein, suggesting that binding is saturated at this concentration. Nevertheless, it is difficult to say that this is indeed the case, because binding interactions occur in the intermediary exchange regime where K_D values cannot be accurately determined.[52] Nevertheless, if binding were to saturate at ~4 μM spike protein with Gal-3 at 20 μM, binding stoichiometry would be ~5 molecules of Gal-3 per 1 molecule of spike protein, and thus ~5 Gal-3 binding sites on the Omicron variant spike protein, a stoichiometry that seems reasonable.

Lactose competes with Gal-3 from binding to SARS-CoV-2 Spike Protein. A reduction in resonance broadening is a good indicator of a reduction in ligand binding when binding occurs in the intermediary exchange regime on the chemical shift time scale. In the absence of lactose, Gal-3 FL (20 μM) resonances in the presence of 4 μM spike protein are highly broadened, consistent with binding of Gal-3 FL to the SARS-CoV-2 S1 spike protein (Figure S2A). In this instance, Gal-3 resonance broadening (ΔINT) is less for residues within the NT and more so for those within the CRD.[40] This is not unusual, because the NT is dynamic and transiently interacts with the F-face of the CRD. ΔINT values

averaged over all residues 1-250 is 0.911, whereas ΔINT values averaged over residues 1-113 (NT) and 114-250 (CRD) are 0.816 and 0.972, respectively.

Addition of 10 mM lactose greatly decreases Gal-3 FL resonance broadening induced by its equilibrium binding to the spike protein S1 domain (Figure S2B). Here, ΔINT values averaged over all residues 1-250, residues 1-113 and residues 114-250 are 0.473, 0.341, and 0.558, respectively, indicating that lactose competes with glycans on the surface of the spike protein for binding to Gal-3 FL. However, it is important to note that the lactose-induced reduction in Gal-3 FL resonance broadening occurs differentially, with some residues showing minimal if any change and others showing a large change (Figure S2B). This differential effect suggests that the Gal-3 glycan-binding epitope on the spike protein involves carbohydrates other than, and in addition to, β-galactosides like lactose. In fact, Lenza et al. reported that Gal-3 can bind to various glycosides on the spike protein RBD.[54]

With truncated Gal-3 CRD (20 μM), binding to the SARS-CoV-2 spike protein S1 (4 μM) is demonstrated by the observed highly broadened CRD resonances (Figure S2C), with the ΔINT averaged over residues 114-250 being 0.898. In this instance, addition of 10 mM lactose greatly decreases Gal-3 CRD resonance broadening differentially throughout the CRD (Figure S2D), with the ΔINT averaged over residues 114-250 being 0.232, considerably less than with the Gal-3 FL. Thus, lactose is more effective at competing off truncated Gal-3 CRD from the spike protein than it is with Gal-3 FL. This also indicates that Gal-3 CRD binding to S1 is weaker than that of Gal-3 FL, because the lactose-induced intensity decrease is greater. Moreover, it appears that the β-galactoside lactose alone competes well with glycans on the surface of the spike protein for binding to truncated Gal-3 CRD. In this regard, the glycan binding profile for truncated Gal-3 CRD appears to be different from that for Gal-3 FL, and indicates that Gal-3 FL (CRD + NT) likely binds to a somewhat different complement of glycans on the spike protein, possibly due to the presence of the NT.

Discussion

SARS-CoV-2 manifested in COVID-19 disease has resulted in a recent global pandemic and concomitant economic hardship.[1,2,4] In the absence of a clinically proven, effective antiviral treatment, the COVID-19 virus has spread around the world, and further efforts are required to develop a safe and clinically effective antiviral drug to combat this disease. Even though the use of vaccines is a proven intervention to combat many infections, including COVID[9,10,13,14], vaccines targeting the antigenic sites of spike protein have had limited efficacy at inhibiting the spread of the virus.[6,55] As the antigenic sites in the virus mutate, community spread of the virus can continue, and global threats from these viruses are unlikely to go away.[3,55] In this regard, we need to identify novel mechanisms in order to block their spread. Viruses bind to sugar chains on ACE2 receptors on host cell membranes and mutations in these receptor binding proteins are less frequent.[26,56] Sugar analogs or receptor sugar analogs that block the host cell sugar chains could potentially be used as drugs capable of overcoming viruses with mutagenic potential in their antigenic sites.[3,55]

Patients with COVID-19 can be treated with corticosteroids, a combination of different antiviral drugs, healing plasma, certain antibiotics, and supportive care.[1,9] However, these treatments are not that successful in preventing disease progression.[2,13,14,57] Therefore, any potential pharmacological candidates that can alleviate disease progression and increase resistance to SARS-CoV-2 and its manifestation COVID-19 are promising. Gal-3 is crucial to the entry of SARS-CoV-2 into cells, and its blockage, therefore, may prevent disease progression. Here, we show that by binding to Gal-3, the carbohydrate PL-M can lower viral load by inhibiting entry of SARS-CoV-2 into Vero cells.[46] Furthermore, in clinical studies with COVID-19 patients, PL-M treatment results in a rapid reduction of viral load and increased viral clearance in the absence of adverse effects.[44,45]

The viral blocking effect of PL-M arises from its binding to Gal-3, thereby inhibiting or attenuating interactions between Gal-3 and the S1 spike protein, thus reducing cell infectivity. PL-M is well tolerated (CC_{50} >100 g/mL) by cells and increases the number of viable cells, likely by stimulating cell proliferation.[46] PL-M effectively inhibits viral entry into cells when it is administered either before or after viral infection. In both instances, PL-M decreases viral load by approximately 100-fold based on viral RNA copy number. Our clinical trials provide evidence that use of PL-M as a Gal-3 antagonist can prevent SARS-CoV-2 viral entry into cells *in vivo*. These trials achieved their primary objective of demonstrating the effect of PL-M on lowering viral infectiousness by blocking the SARS-CoV-2 S1 spike protein from promoting viral entry into cells. Moreover, the increase in CT values at the early stage of disease pathogenesis means that further clinical research should be pursued at an even earlier stage to see if PL-M is effective as a prophylactic.

Several investigations have revealed that the sugar binding site on Gal-3 is crucial to its function.[58] Inhibition of this site is likely the key mechanism behind anti-SARS-CoV-2 action of the PL-M polysaccharide. Our NMR structural studies indicate that PLM binds specifically to Gal-3 in the μM range. In relation to Gal-3 inhibitors, it is plausible that PL-M interacts with Gal-3 in the same way as does the structurally similar NTD of the glycosylated S1 subunit of SARS-CoV-2. Overall, PL-M inhibition of Gal-3, as well as blockade of the S1 NTD and ACE2 receptors, may account for the prospective anti-SARS-CoV-2 action of PLM.

Recently, Lenza et al. published an excellent NMR study on the binding of the RBD S1 domain to three galectins: truncated Gal-3 CRD, Gal-7 (which only has a CRD that can dimerize), and the N-terminal CRD of Gal-8.[54] These authors reported that the Gal-3 CRD binds the most strongly to the S1 protein, vis-à-vis Gal-7 or Gal-8 N-terminal CRDs. This is one reason why we focused our study on Gal-3 alone. Overall, both studies are consistent in terms of sugar binding to the CRD S-face being important for binding interactions with the S1 protein. This is not surprising, because it is known that Gal-3 interacts with glycans on the S1 protein.

Lenza et al. used resonance broadening as a signature for binding, and whereas this parameter indeed reflects binding, it is not usually that straight forward to infer where the binding epitope is, primarily because of indirect events with e.g. changes in internal motions and allosteric effects.[54] It was surprising that Lenza et al. did not show chemical shift changes from Gal-3 CRD upon binding S1, because these are more informative of environmental changes that occur upon binding, as well as for the binding epitope.[54] We looked at both, and our broadening data (Figure 4B) indeed indicate binding. In fact, comparison of resonance broadening between full length Gal-3 and truncated Gal-3 CRD (used solely in Lenza et al.[54]), clearly shows that S1 binds more strongly to the CRD in full length Gal-3 (CRD plus the long, aperiodic NT) and that the Gal-3 NT and CRD F-face are also somehow involved in interactions with the S1 protein. Chemical shift changes (Figure 4D) show that whereas the canonical sugar binding site on the CRD S-face is significantly perturbed, so is the F-face on the opposing β-sandwich β-sheet, as well as the NT. Ippel et al. previously showed that the NT transiently binds to the CRD F-face and that this interaction is crucial to the function of full length Gal-3.[40] The Gal-3 CRD can bind to glycans, but it is otherwise relatively inactive. Our data indicate that S1 protein interactions with Gal-3 appear to be mediated both by glycan binding to the CRD S-face, as well as by interactions with the CRD F-face and NT. Alternatively, it could be that S1 interactions with the F-face displace the NT, thus accounting for spectral changes to residues within the NT.

Furthermore, even though both our and their RBDs were expressed in cultured (human embryonic kidney) HEK 239F cells and thus both of our S1 proteins were glycosylated, Lenza et al.[54] used the RBD spike protein S1 domain from the alpha variant B.1.1.7, and we used the S1 protein from the Omicron variant B.1.1.529. The Omicron variant has the most mutations (15 mutations) of any other SARS-CoV-2 variant, and shows enhanced cell entry, making it ~10-fold more virulent (in infectivity) than other variants. This relatively large number of mutations could promote large conformational alterations that enhance interactions with the ACE2 receptor on the cell surface[59], more so than the alpha variant. It is perhaps more important to note that the molar ratio of Gal-3:S1 (Omicron) that our study used was 20:1 (i.e. Gal-3 at 20 μM and S1 at 1 μM or less), whereas Lenza et al. with the alpha variant used a ratio of 1:1 (Gal-3 at 60 μM) to 1:0.4.[54] Therefore, the fact that we used much less S1 and yet had similar magnitude NMR spectral changes to those reported by Lenza et al.[54], indicates that Gal-3 binds much more strongly to the Omicron S1 protein than to the alpha variant S1 protein. This is consistent with the greater infectivity of the Omicron variant, and appears to relate the strength of Gal-3 binding to the S1 protein to increased SARS-CoV-2 viral infectivity from Omicron vis-à-vis Alpha.

Conclusions

The SARS-CoV2 spike glycoprotein plays a key role in the virus's cellular attachment and entry processes. The S1-NTD of SARS-CoV2 is structurally and sequentially similar to human Gal-3. Our findings shed light on the efficacy of PL-M against SARS-CoV-2 infection, as well as its antiviral mechanism of action. PL-M reduces viral load and increases viral clearance in patients with mild to severe COVID-19. In addition to exploring the clinical efficacy of PL-M, NMR investigations show that Gal-3 has a high affinity for PL-M, as well as for the spike protein S1. In this regard, PL-M inhibits SARS-CoV-2 entry into cells by antagonizing Gal-3 binding to the viral spike protein. Due to its significant efficacy and tolerability, PL-M has the potential to be used in the treatment and prevention of COVID-19, and perhaps of other corona viruses. Our glycovirology approach has been successful in developing a therapeutic strategy to block viral entry into cells and thereby attenuate severity from COVID-19, and because there is a paucity of therapeutics to treat COVID-19[25], developing an agent like PL-M is paramount in treating the disease.

Conflicts of Interest. A.S. and D.P. are employees of Pharmalectin and hold shares in the company.

Funding. Pharmalectin, Inc. has funded the studies reported in this manuscript.

References

1. Acosta RAH, Garrigos ZE, Marcelin JR. COVID-19 pathogenesis and clinical manifestations. *Infect Dis Clin N Am*. 2022;36:231-249.
2. World Health Organization. *COVID-19 vaccine tracker and landscape*, 2022.
3. Harvey WT. SARS-CoV-2 variants, spike mutations and immune escape. *Nature Rev Microbiol*. 2021;19:409-424.
4. Bano I, Sharif M, Alam S. Genetic drift in the genome of SARS CoV-2 and its global health concern. *J Med Virol*. 2022;94:88-98.
5. Khandia, R. Emergence of SARS-CoV-2 Omicron (B.1.1.529) variant, salient features, high global health concerns and strategies to counter it amid ongoing COVID-19 pandemic. *Environ Res*. 2022;209:112816, doi:10.1016/j.envres.2022.112816.
6. Chi X, Yan R, Zhang J, Zhang G, Zhang Y, Hao M, Zhang Z, Fan P, Dong Y, Yang Y. A neutralizing human antibody binds to the N-terminal domain of the Spike protein of SARS-CoV-2. *Science* 2020;369:650–655.
7. Behloul N, Baha S, Shi R, Meng J. Role of the GTNGTKR motif in the N-terminal receptor-binding domain of the SARS-CoV-2 spike protein. *Virus Res*. 2020;286:198058, doi:10.1016/j.virusres.2020.198058.
8. Wang J, Jiang M, Chen X, Montaner LJ. Cytokine storm and leukocyte changes in mild versus severe SARS-CoV-2 infection: Review of 3939 COVID-19 patients in China and emerging pathogenesis and therapy concepts. *J Leukoc Biol*. 2020;108:17-41.
9. Aleem A, Samad A, Vaqar S. Emerging Variants of SARS-CoV-2 and Novel Therapeutics Against Coronavirus (COVID-19). *Stat Pearls*. Treasure Island (FL) 2024; PMID: 34033342.
10. Haslwanter D, Dieterle ME, Wec AZ, O'Brien CM. A combination of receptor-binding domain and N-terminal domain neutralizing antibodies limits the generation of SARS-CoV-2 spike neutralization-escape mutants. *Mbio* 2021;12:doi.org/10.1128/mbio.02473.
11. Wang C, Wang Z, Wang G, Johnson Y-NL, Zhang K, Li W. COVID-19 in early 2021: current status and looking forward. *Signal Transduc Targeted Ther*. 2021;6:1-14.
12. Singanayagam A, Hakki S, Dunning J, Madon KJ, Crone MA, Koycheva A, Derqui-Fernandez N, Barnett JL, Whitfield MG, Varro R. Community transmission and viral load kinetics of the SARS-CoV-2 delta (B.1.617.2) variant in vaccinated and unvaccinated individuals in the UK: a prospective longitudinal cohort study. *Lancet Infect Dis*. 2022;22:183-195.
13. Eyre DW, Taylor D, Purver M, Chapman D, Fowler T, Pouwels KB, Walker AS, Peto TEA. Effect of Covid-19 vaccination on transmission of alpha and delta variants. *New Engl J Med*. 2022;386:744-756.
14. de Gier B, Andeweg S, Backer JA, Hahné SJ, van den Hof S, de Melker HE, Knol MJ. Vaccine effectiveness against SARS-CoV-2 transmission to household contacts during dominance of Delta variant (B. 1.617. 2). *Eurosurveillance* 2021;26:2100977.
15. Li F. Receptor recognition mechanisms of coronaviruses: A decade of structural studies. *J. Virol*. 2015;89:1954–1964.
16. Cui J, Li F, Shi Z-L. Origin and evolution of pathogenic coronaviruses. *Nature Rev. Microbiol*. 2019;17:181-192.
17. Tortorici MA. Structural basis for human coronavirus attachment to sialic acid receptors. *Nat Struct Mol Biol*. 2019;26:481-489.
18. Gong Y, Qin S, Dai L, Tian Z. The glycosylation in SARS-CoV-2 and its receptor ACE2. *Signal Transduc Targeted Ther*. 2021;6:396.
19. Mousavizadeh L, Ghasemi S. Genotype and phenotype of COVID-19: Their roles in pathogenesis. *J Microbiol Immunol Infect*. 2021;54:159-163.
20. Sivaraman H, Er SY, Choong YK, Gavor E, Sivaraman J. Structural basis of SARS-CoV-2–and SARS-CoV–receptor binding and small-molecule blockers as potential therapeutics. *Ann Rev Pharmacol Toxicol*. 2021;61:465-493.
21. Xia S, Liu M, Wang C, Xu W. Inhibition of SARS-CoV-2 (previously 2019-nCoV) infection by a highly potent pan-coronavirus fusion inhibitor targeting its spike protein that harbors a high capacity to mediate membrane fusion. *Cell Res*. 2020;30:343–355.
22. Díaz-Alvarez L, Ortega E. The Many Roles of Galectin-3, a Multifaceted Molecule, in Innate Immune Responses against Pathogens. *Mediators Inflamm*. 2017;9247574, doi:10.1155/2017/9247574.
23. Machala EA, McSharry BP, Rouse BT, Abendroth A, Slobedman B. Gal power: The diverse roles of galectins in regulating viral infections. *J. Gen. Virol*. 2019;100:333-349.
24. Wang WH, Lin CY, Chang MR, Urbina AN, Assavalapsakul W, Thitithanyanont A, Chen YH, Liu FT, Wang SF. The role of galectins in virus infection - A systemic literature review. *J Microbiol Immunol Infect*. 2020;53:925-935.
25. Caniglia JL, Asuthkar S, Tsung AJ, Guda MR, Velpula KK. Immunopathology of galectin-3: an increasingly promising target in COVID-19. *F1000Res* 2020;9:1078, doi:10.12688/f1000research.25979.2.
26. Lee Y-K. Carbohydrate Ligands for COVID-19 Spike Proteins. *Viruses* 2022;14: doi:10.3390/v14020330.
27. Sato S, St-Pierre C, Bhaumik P, Nieminen J. Galectins in innate immunity: dual functions of host soluble beta-galactoside-binding lectins as damage-associated molecular patterns (DAMPs) and as receptors for pathogen-associated molecular patterns (PAMPs). *Immunol Rev*. 2009;230:172-187.
28. Del Valle DM, Kim-Schulze S, Huang H-H, Beckmann ND, Nirenberg S, Wang B, Lavin Y. An inflammatory cytokine signature predicts COVID-19 severity and survival. *Nature Med*. 2020;26:1636-1643.
29. Zhang C, Wu Z, Li J, Zhao H, Wang GQ. Cytokine release syndrome in severe COVID-19: interleukin-6 receptor antagonist tocilizumab may be the key to reduce mortality. *Int J Antimicrob Agents* 2020;55: doi:10.1016/j.ijantimicag.2020.105954.
30. Cervantes-Alvarez E, la Rosa NL, la Mora MS, Valdez-Sandoval P, Palacios-Jimenez M, Rodriguez-Alvarez F, Vera-Maldonado BI, Aguirre-Aguilar E, Escobar-Valderrama JM, Alanis-Mendizabal J. Galectin-3 as a potential prognostic biomarker of severe COVID-19 in SARS-CoV-2 infected patients. *Sci Rep*. 2022;12:1856.

31. Kulkarni R, Prasad A. Exosomes derived from HIV-1 infected DCs mediate viral trans-infection via fibronectin and galectin-3. *Sci. Rep.* 2017;7:1-14.
32. Okamoto M, Hidaka A, Toyama M, Baba M. Galectin-3 is involved in HIV-1 expression through NF-κB activation and associated with Tat in latently infected cells. *Virus Res.* 2019;260:86-93.
33. Dumic J, Dabelic S, Flögel M. Galectin-3: An open-ended story; Review. *Biochim Biophys Acta* 2006;1760:616 – 635.
34. Zhao Z, Xu X, Cheng H, Miller MC, He Z, Gu H, Zhang Z, Raz A, Tai G, Mayo KH, Zhou Y. Galectin-3 N-terminal tail prolines modulate cell activity and glycan-mediated oligomerization/phase separation. *Proc Natl Acad Sci USA.* 2021;118:doi: 10.1073/pnas.2021074118).
35. Nesmelova IV, Dings RPM, Mayo KH. Understanding galectin structure-function relationships to design effective antagonists, Chapter 2 in "Galectins" (ed., Klyosov, A.) 2008 Oxford University Press, New York.
36. Barondes SH, Castronovo V, Cooper DNW, Cummings RD. Galectins: A Family of Animal b-Galactoside Binding Lectins. *Cell* 1994;76:597-596.
37. Mayo KH. Galectins: From theory to therapy. *IDrugs* 2008;11:97-100.
38. Miller MC, Ribeiro JP, Roldós V, Martín-Santamaría S, Cañada FJ, Nesmelova IA, André S, Pang M, Klyosov AA, Baum LG, Jiménez-Barbero J, Gabius H-J, Mayo KH. Structural aspects of binding of a-linked digalactosides to human galectin-1. *Glycobiol.* 2011;21:1627-1641.
39. Miller M, Nesmelova IV, Klyosov A, Platt D, Mayo KH. The carbohydrate binding domain on galectin-1 is more extensive for a complex glycan than for simple saccharides: implications for galectin-glycan interactions at the cell surface. *Biochem J.* 2009a;421:211-221.
40. Ippel H, Miller MC, Vértesy S, Zheng Y, Cañada FJ, Suylen D, Umemoto K, Romano C, Hackeng T, Tai G, Leffler H, Kopitz J, André S, Kübler D, Jiménez-Barbero J, Oscarson S, Gabius H-J, Mayo KH. Intra- and intermolecular interactions of human galectin-3: assessment by full-assignment-based NMR. *Glycobiol.* 2016;26:888-903.
41. Miller MC, Klyosov A, Mayo KH. The a-galactomannan Davanat binds galectin-1 at a site different from the conventional galectin carbohydrate binding site. *Glycobiol.* 2009b;19:1034-1045.
42. Miller MC, Klyosov A, Mayo KH. Structural Features for a-galactomannan binding to galectin-1. *Glycobiol.* 2012;22:543-551.
43. Miller MC, Ippel H, Suylen D, Klyosov AA, Traber PG, Hackeng T, Mayo KH. Binding of Polysaccharides to Human Galectin-3 at a Non-Canonical Site in its Carbohydrate Recognition Domain. *Glycobiol.* 2016;26:88-99.
44. Sigamani A. Galectin antagonist use in mild cases of SARS-CoV-2; pilot feasibility randomised, open label, controlled trial. *medRxiv.* 2020;doi:10.1101/2020.12.03. 20238840.
45. Sigamani A, Mayo KH, Miller MC, Chen-Walden H, Reddy S, Platt D. An Oral Galectin Inhibitor in COVID-19-A Phase II Randomized Controlled Trial. *Vaccines* 2023;11:731-739.
46. Sigamani A, Chen-Walden H, Pahan J, Miller MC, Mayo KH, Platt D. Carbohydrate prolectin-M, a galectin-3 antagonist, blocks SARS-CoV-2 activity. *Intern J Health Sci.* 2022;6:6671–6683.
47. Portacci A, Diaferia F, Santomasi C, Dragonieri S, Boniello E, Di Serio F, Carpagnano GE. Galectin-3 as prognostic biomarker in patients with COVID-19 acute respiratory failure. *Respir Med.* 2021;187:106556.
48. Milanetti E. In-Silico Evidence for a Two Receptor Based Strategy of SARS-CoV-2. *Front Mol Biosci.* 2021;8:690655, doi:10.3389/fmolb.2021.690655.
49. Delaglio F. NMRPipe: a multidimensional spectral processing system based on UNIX pipes. *J Biomol NMR* 1995;6:277-293.
50. Johnson BA, Blevins RA. NMR View: A computer program for the visualization and analysis of NMR data. *J. Biomol. NMR* 1994;4:603-614.
51. Ippel H, Miller MC, Berbis MA, Suylen D, Andre S, Hackeng TM, Canada FJ, Weber C, Gabius H-J, Jimenez-Barbero J, Mayo KH. ^{1}H, ^{13}C, and ^{15}N backbone and side-chain chemical shift assignments for the 36 proline-containing, full length 29 kDa human chimera-type galectin-3. *Biomol NMR Assign.* 2015;9:59-63.
52. Williamson MP. Using chemical shift perturbation to characterise ligand binding. *Prog Nucl Magn Reson Spectrosc.* 2013;73:1-16.
53. Seetharaman J, Kanigsberg A, Slaaby R, Leffler H, Barondes SH, Rini JM. X-ray Crystal Structure of the Human Galectin-3 Carbohydrate Recognition Domain at 2.1-Å Resolution. *J Biol Chem.* 1998;273:13047-13052.
54. Lenza MP, Oyenarte I, Diercks T, Quintana JI, Gimeno A, Coelho H, Diniz A, Peccati F, Delgado S, Bosch A, Valle M, Millet O, Abrescia NGA, Palazón A, Marcelo F, Jiménez-Osés G, Jiménez-Barbero J, Arda A, Ereno-Orbea. Characterization of N-Linked Glycans in the Receptor Binding Domain of the SARS-CoV-2 Spike Protein and their Interactions with Human Lectins. *Angew Chem Int Ed.* 2020;59:23763 – 23771.
55. Lam SD, Waman VP, Orengo C, Lees J. Insertions in the SARS-CoV-2 Spike N-Terminal Domain May Aid COVID-19 Transmission. *bioRxiv.* 2021;1021.2012.2006. 471394, doi:10.1101/2021.12.06.471394.
56. Shin HJ, Ku KB, Kim HS, Moon HW, Jeong GU, Hwang I, Yoon GY, Lee S, Lee S, Ahn D-G, Kim K-D, Kwon Y-C, Kim B-T, Kim S-J, Kim C. Receptor-binding domain of SARS-CoV-2 spike protein efficiently inhibits SARS-CoV-2 infection and attachment to mouse lung. *Int J Biol Sci.* 2021;17:3786-3794.
57. England, J. T. Weathering the COVID-19 storm: Lessons from hematologic cytokine syndromes. *Blood Rev.* 2021;45:100707, doi:10.1016/j.blre.2020.100707.
58. Di Lella S. When galectins recognize glycans: from biochemistry to physiology and back again. *Biochem.* 2011;50:7842-7857.
59. Zhang X, Wu S, Wu B, Yang Q, Chen A, Li Y, Zhang Y, Pan T, Zhang H, He X. SARS-CoV-2 Omicron strain exhibits potent capabilities for immune evasion and viral entrance. *Signal Transduc Targeted Ther.* 2021;6:430; doi.org/10.1038/s41392-021-00852-5.

60. Miller MC, Cai C, Wichapong K, Bhaduri S, Pohl NLB, Linhardt R, Gabius H-J, Mayo KH. Structural insight into the binding of human galectins to corneal keratan sulfate, its desulfated form and related saccharides. *Sci Reports* 2020;10:15708. doi: 10.1038/s41598-020-72645-9.

61. Zheng Y, Su J, Miller MC, Zhang T, Mayzel M, Tai G, Mayo KH, Zhou Y. Topsy-turvy binding of negatively-charged homogalacturonan oligosaccharides to galectin-3. *Glycobiol*. 2021;31:341-350.